STUDY OF IEEE 802.11 WIRELESS NETWORKS IN HARSH ENVIRONMENT

Kaustubh Phanse [1] Mohammad-Reza Akhavan [2] Ulf Olsson [3]

[1] Department of Computer Science and Electrical Engineering, Luleå University of Technology, SE 97187 Luleå, Sweden. E-mail: kphanse@ltu.se Phone: +46 (0)920 491428

[2] Department of Computer Science and Electrical Engineering, Luleå University of Technology, SE 97187 Luleå, Sweden. E-mail: akhavan@ludd.ltu.se

[3] LKAB, SE 98186 Kiruna, Sweden. E-mail: ulf.olsson@lkab.com Phone: +46(0)980 71036

ABSTRACT

IEEE 802.11 technologies are expected to remain the popular wireless local area networking solution for home and office environments. With growing interest within the process and manufacturing industry to go wireless, these technologies are a natural choice for enabling tetherless control and maintenance. However, the use of IEEE 802.11 suite of protocols for wireless access in unconventional, harsh environments is limited and their behavior and performance in these settings is not yet well understood. A prime example of such a setting is the LKAB underground iron-ore mine in Kiruna, Sweden. LKAB envisions an economical and effective wireless access solution in the mines for increasing automation, e.g., remotely control mining equipment such as mobile loading machines and drilling equipment. In this paper, we present our experiences of operating an IEEE 802.11g based wireless network in the LKAB underground iron-ore mine. Using measurements, we characterize and model the environment and its effect on the performance of higher layer protocols. We derive the theoretical limits of IEEE 802.11g and compare them with our experimental results. We observe a highly reflective environment in the mine, which causes multipath fading and in turn, considerably degrades the maximum achievable throughput in practice.

KEYWORDS

IEEE 802.11, wireless, iron-ore mine, measurements, fading, interference, throughput, theoretical

1. INTRODUCTION

The process and manufacturing industry views wireless technology as one of the key enablers for realizing innovations such as process automation, agile manufacturing, and remote monitoring and maintenance.

One wireless technology that has attracted considerable attention within the process and manufacturing industry is the IEEE 802.11 protocol suite. This is natural due to the immense success achieved by IEEE 802.11 as the popular broadband wireless local-area networking solution in home/office environment and the availability of cheap, commercial-off-the-shelf (COTS) 802.11 products. The use of IEEE 802.11 protocols for wireless access in industrial environment is, however, limited and their behavior and performance in these settings is not yet well understood. We argue that industrial environments generally offer more challenging conditions (e.g., higher radio interference) as compared to conventional home/office environment envisioned for 802.11 deployments, and a study with real-life testing is important before adopting a wireless technology in such unconventional settings.

In this paper, we present a case study of one such environment: operating IEEE 802.11g based wireless networks in the LKAB underground iron-ore mine in Kiruna, Sweden. LKAB envisions an economical and effective wireless access solution in the mines for increasing automation, e.g., remotely control mining equipment such as mobile loading machines and drilling equipment. The wireless network, to be integrated into a Gigabit Ethernet backbone, should offer high bandwidth and quality of service enabling support for a heterogeneous mix of traffic such as voice over IP, interactive video, real-time control traffic, sensor data and non-real time traffic generated by the web-based control and maintenance applications. As a first step, we conduct an experimental study using IEEE 802.11g (IEEE standard, 2003). The aim of our experiments is two-fold: first, to model the radio propagation conditions in the underground iron-ore mines; and second, to measure the network performance in terms of higher layer protocol metrics such as throughput, delay and packet loss.

The rest of the paper is organized as follows. In Section 2, we discuss our experimental methodology and the scenarios considered for measurements. We present our experimental results in Section 3. In Section 4, we derive the theoretical performance limits for 802.11g under ideal conditions. Finally, Section 5 presents our concluding remarks.

2. EXPERIMENTAL METHODOLOGY AND SET-UP

The experiments were conducted in a section of LKAB's underground iron-ore mines. A top view of the work area is shown in Figure 1; it represents a typical production area that is to be supported using wireless technology such as IEEE 802.11. We installed IEEE 802.11g access points (APs) along the field tunnel, at the entrance of each tunnel. Using a backbone switch, we controlled the access points allowing us to conduct experiments with a single active AP as well as up to six active APs. A computer connected to the switch was used to generate data traffic to be transmitted over the 802.11g access network. IEEE 802.11g is a relatively new standard that is backward compatible with older IEEE 802.11b standard. In our experiments, we used both modes of operation: a *g-only mode* (i.e., only 802.11g clients are supported) or in a *b/g mode* (i.e., both 802.11g and 802.11b clients are supported). The backward compatibility comes at the expense of slightly lower performance for 802.11g clients; for further details, we refer the readers to (IEEE standard, 2003).

The experiments were divided into two sets: (1) *channel modeling*: with focus on modeling the behavior of the channel conditions; and (2) *higher layer performance*: with focus on measuring higher layer protocol performance in terms of metrics such as throughput, delay and packet loss.

2.1 Channel modeling

Two different equipments were used: a spectrum analyzer with an antenna and S-band antenna amplifier with a 30 dB gain and a laptop with a Linksys 802.11g wireless card. A freeware called *Netstumbler* was used to measure the signal strength. This entire set-up was installed on a vehicle that enabled us to measure channel conditions at different locations in the tunnels. While the spectrum analyzer was inside

the vehicle, the antenna was located high on top of the backdoor of the vehicle to ensure line of sight with the AP. During actual production, the mobile loaders and drilling rigs are expected to operate in similar conditions.

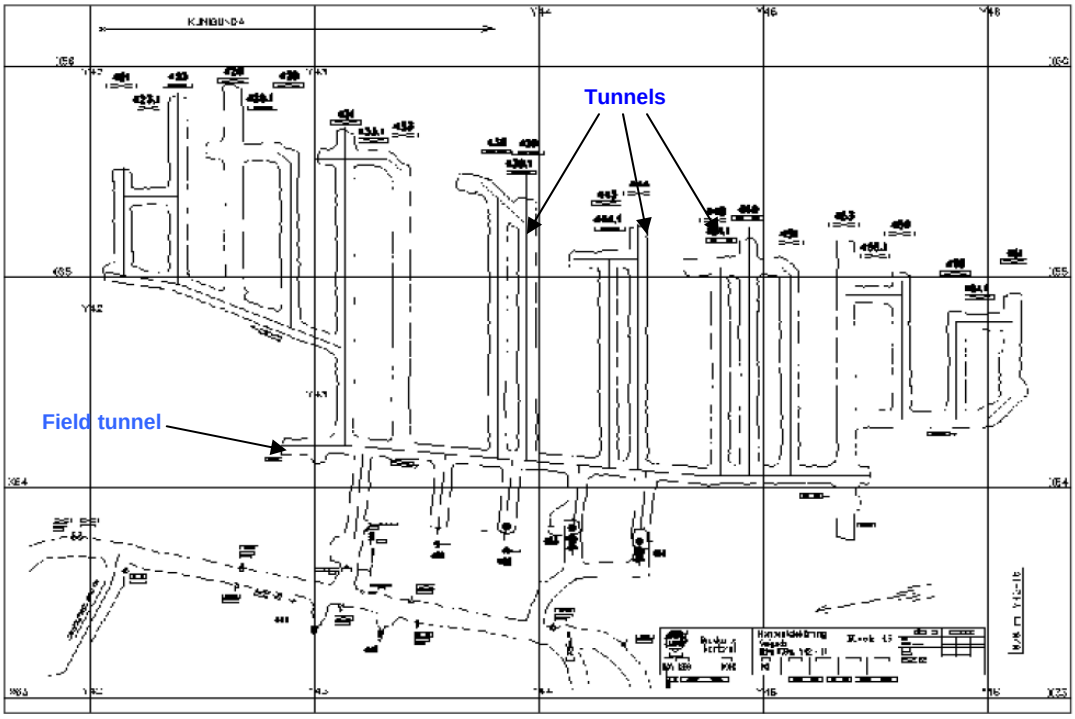

Figure 1: Map (top view) of the work area in the LKAB underground iron-ore mine

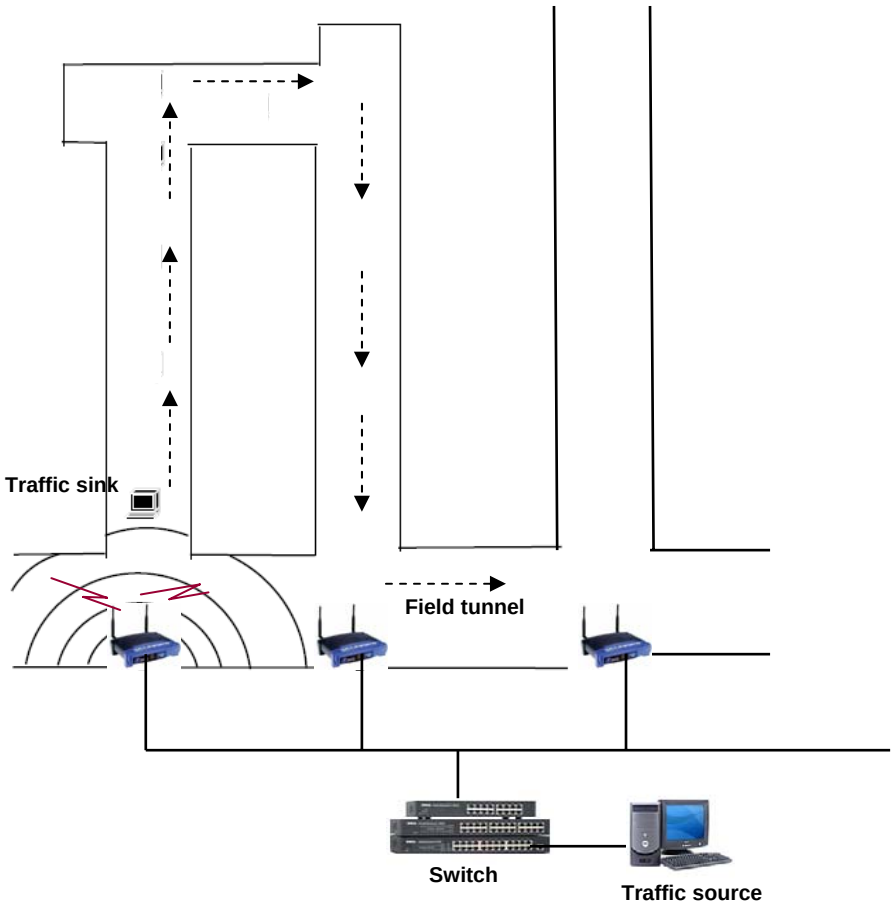

Figure 2: Experimental scenario 1 with single active access point; dotted arrows indicate movement of the vehicle carrying the wireless client (traffic sink) and spectrum analyzer.

2.2 Higher layer performance

We used a traffic generating software called *Iperf* to send data traffic using the computer connected to the backbone switch. Our focus was on measuring the throughput and delay limits of the 802.11 network and packet loss ratio. So we avoided the congestion and flow control of the transmission control protocol (TCP), and used the user datagram protocol (UDP) for data transport. A Linux-based computer running the *Iperf* server was used as a traffic-sink to receive the generated data over the 802.11 network. On the same computer, we used *Tcpdump* to measure the network performance and used the *Trpr* and *Gnuplot* tools to plot the graphs. To repeat the experiments several times and measure average performance, we automated the traffic generation and measurement processes using scripts.

2.3 Experimental scenarios

Broadly, two scenarios were considered in our experiments.
(1) *Only one AP active (Figure 2)*: the aim was to measure the coverage inside the tunnel facing the access point and the coverage in the field tunnel; and
(2) *Several APs active*: the aim was to measure the effect of interference from overlapping AP coverage with all other settings similar to scenario 1.

3. RESULTS

In this section, we present the results from our experiments.

3.1 Channel modeling

Even in presence of a single access point (AP), considerable amount of the interference was observed at the receiver. The high metal content in the walls, floors and ceiling of the tunnels led to a highly reflective environment. This in turn was the cause for signal reflection, scattering and multi-path fading, where several copies of the signal interfere at the receiver. Due to the intense and unpredictable interference in the mine it was difficult to exactly measure how the signals behave; for instance, we were unable to plot the channel impulse response.

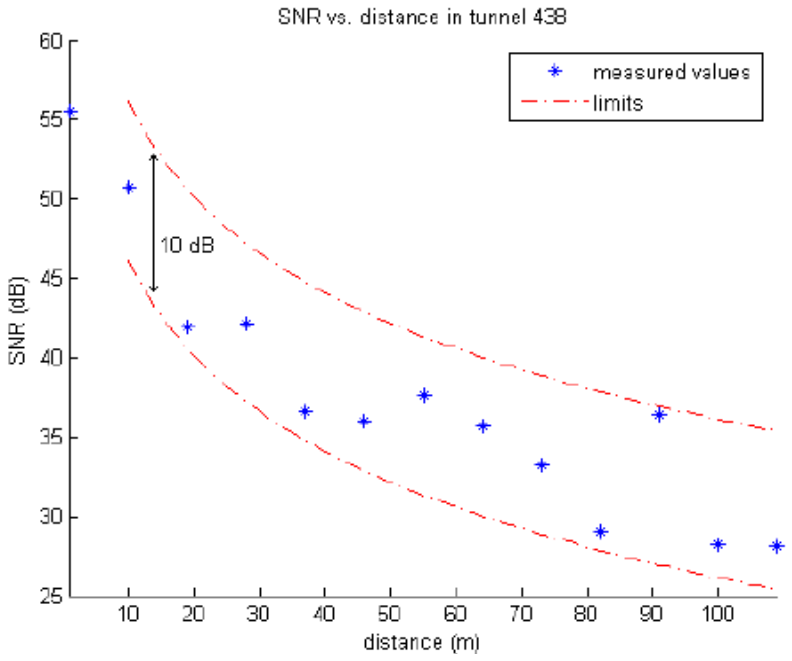

Figure 3: SNR as a function of the distance from the access point.

In Figure 3, we plot the measured signal-to-noise ratio (SNR) as a function of distance from the AP as we move further into the tunnel. In the free-space path loss model (Rappaport, 2001), the SNR is expected to decrease at least as square of the distance from the wireless transmitter. This is indicated by the upper limit. The lower limit corresponds to a path loss exponent n = 3, comparable to typical indoor office environments (Henty, 2001). It is noteworthy that initially the SNR decreases much rapidly, while as we approach the end of the tunnel the SNR exhibits erratic behavior, increasing and decreasing radically. The increase in SNR is attributed to the reflection of the signal from the tunnel walls. The maximum increase in the SNR (about 90 m from the AP and less than 10 m from the tunnel end) occurs due to strong reflections from the end-of-the-tunnel wall. The last two values are from measurements taken as we turn into the adjoining tunnel and lose line-of-sight with the AP. The behavior was similar in other tunnels.

We validated the signal reflection characteristics by measuring the SNR at about the same distance from the AP, but by moving sideways in the tunnel. As shown in Figure 4, the SNR was found to increase as we moved close to the walls on both sides of the tunnel. The highly reflective nature of the environment (due to extreme metal content and structure of production area) leads to considerable multipath fading, i.e., several copies of the signal following different paths and with different delays reach the receiver. As illustrated in Figure 5, if the delay spread from the multiple copies of the signal is comparable or greater than the symbol duration, it causes inter-symbol interference resulting in irreducible packet errors at the receiver. As will be seen from results in Section 3.2, this considerably limits the maximum achievable data throughput in practice.

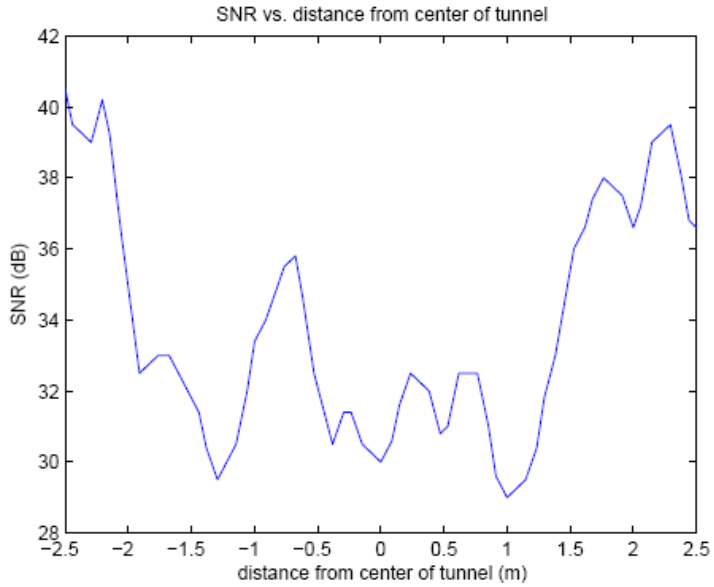

Figure 4: Effect of the proximity to the tunnel walls on SNR.

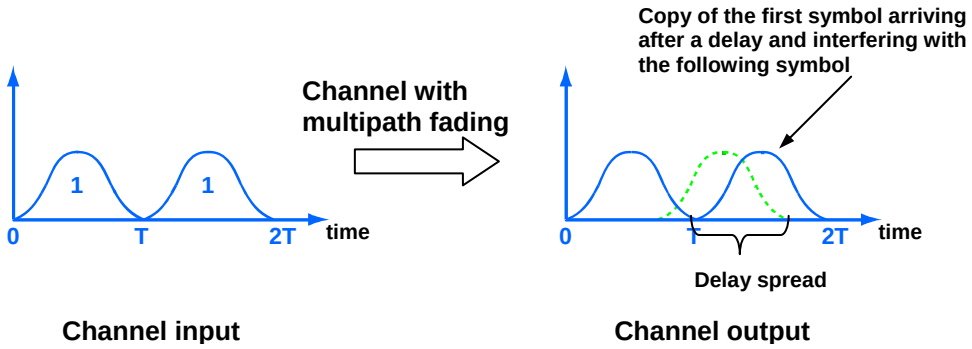

Figure 5: Illustration of multipath fading and delay spread causing inter-symbol interference.

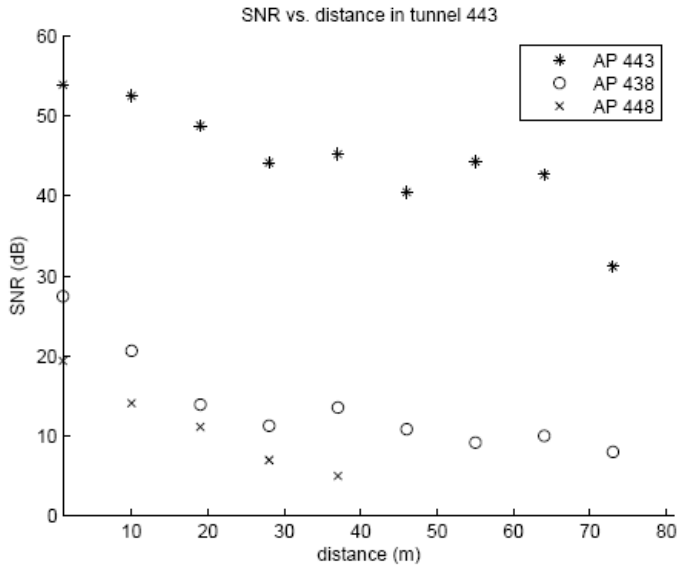

Figure 6: Coverage of three adjoining APs in tunnel 443.

We conducted measurements with three access points active, using non-overlapping channels, at three adjoining tunnels: 438, 443, and 448. Measurements were taken in tunnel 443. In addition to the tunnel's own AP the other two APs were visible in the tunnel. The SNR from the three APs is shown in Figure 6. Without line-of-sight, the signal from adjoining APs is weak and dies down quickly as we move further into the tunnel.

3.2 Higher layer performance

In the first set of experiments, we measured the performance of a UDP-based application in terms of throughput, delay and packet loss as a function of the packet size and distance from the AP. We used different packet sizes in the range from 128 bytes to 1470 bytes. Preliminary tests showed that with a packet size of 1470 bytes, the maximum throughput obtained was about 4 Mbps with minimal (less than 5%) packet loss. Hence, we decided to load the network with application data rate of 4 Mbps. We repeated each experiment five times in different tunnels for computing average performance. During an experiment, only one access point was active and measurements were made in the tunnel facing or in line-of-sight with the AP.

Packet size (bytes)	**Average performance (b/g mode)**		**Average performance (g-only mode)**	
	Throughput (Mbps)	**Packet loss (%)**	**Throughput (Mbps)**	**Packet loss (%)**
1470	2.5 – 3.7	0 – 5	3.7 – 3.8	0 – 1
1024	2.5 – 3.5	5 – 10	3.6 – 3.8	0 – 3
512	1.5 – 2.5	5 – 10	3.5 – 3.7	3 – 7
256	1 – 2	8 – 20	3.1 – 3.6	4 – 16
128	0.75 – 1.5	35 – 45	2.6 – 3.6	5 – 30

Table 1: Average performance of a UDP based application in *b/g* and *g-only* modes.

The measurement results are shown in Table 1. The performance degrades considerably with decrease in packet size. Smaller packet size results in greater overhead: more control bytes per data byte and more time spent in trying to gain access to the shared wireless medium (for details, see the following section on *theoretical limits*). As we moved further into a tunnel, throughput decreased and packet loss increased with increase in distance from the AP during the first 50-60 meters. However, as we approached the end

of the tunnel, the throughput increased and packet loss decreased. This is attributed to the increased SNR due to reflection, as discussed in our previous results. The performance of the *g-only mode* was found to be better than the *b/g mode* as expected, due to less overhead. In general, the variance of the measured values was high portraying the random nature of the environment. In addition, we also measured the end-to-end delay. For the *b/g mode*, the average end-to-end delay was less than 5 ms in all cases. For the *g-only mode*, the average end-to-end delay was less than 0.8 ms. The average values for delay do not account for packets that were lost, and hence does not reflect the unreliable nature of the wireless channel.

In addition to the average performance for individual tunnels, we were also interested in measuring the effect of different access point configurations on the coverage in the entire work area. Three different configurations were tested: (1) two APs at two ends of the field tunnel and operating on non-overlapping channels 1 and 11; (2) three APs equally distributed along the field tunnel and operating on non-overlapping channels 1, 6 and 11; and (3) three APs equally distributed along the field tunnel with two APs operating on same channel 1 and the third AP operating on non-overlapping channel 11. The client computer moved through the various tunnels. The results for the three scenarios are shown in Figures 7, 8 and 9, respectively. It is evident that two APs are not sufficient to cover the work area with the client repeatedly finding itself outside the coverage (Figure 7). With three APs operating on non-overlapping channels, the coverage is improved considerably (Figure 8). However, when two of those APs are made to operate on the same channel, the interference severely degrades the performance (Figure 9).

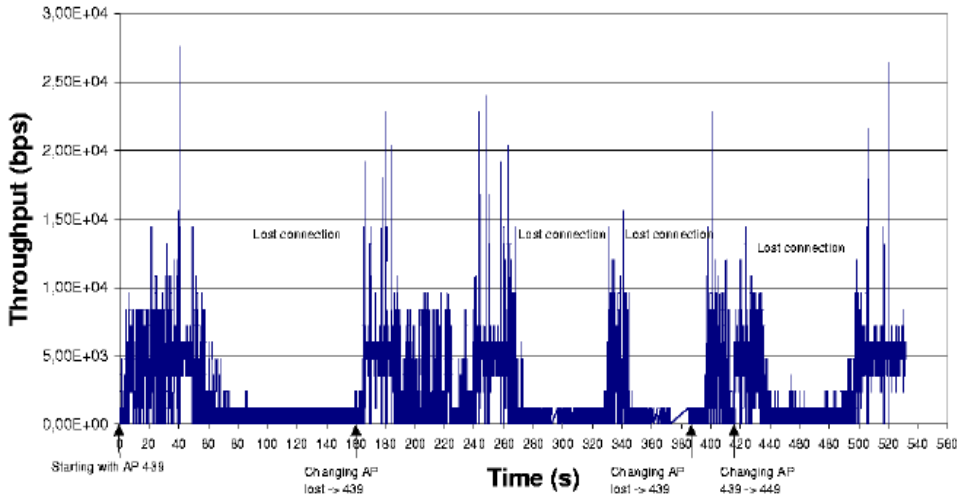

Figure 7: Observed application throughput in presence of two APs using non-overlapping channels 1 and 11 deployed along the field tunnel.

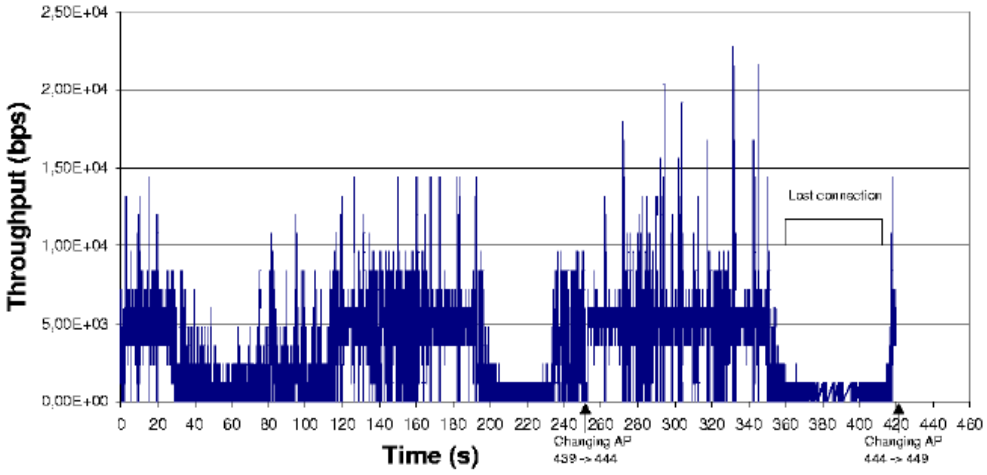

Figure 8: Observed application throughput in presence of three APs using non-overlapping channels 1, 6, and 11 deployed along the field tunnel.

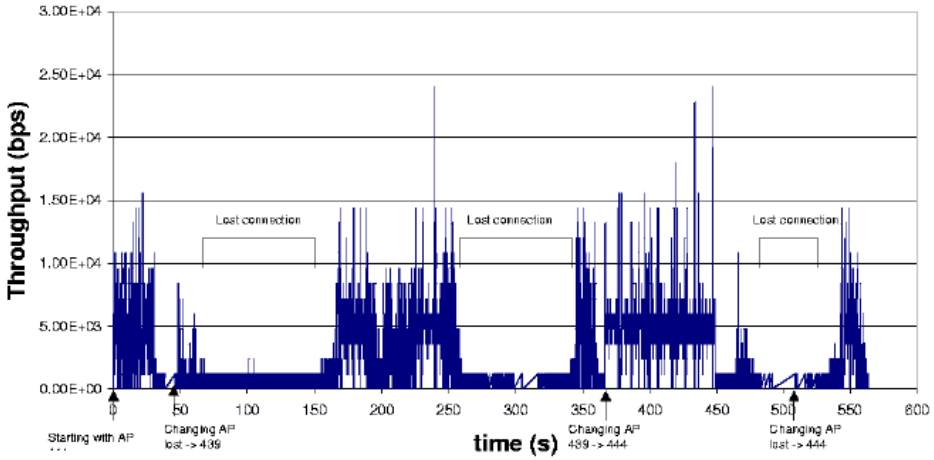

Figure 9: Observed application throughput in presence of three APs using channels 1, 11 and 1 respectively, deployed along the field tunnel.

3.3 Theoretical Limits of IEEE 802.11g

In this section, we derive the theoretical limits of IEEE 802.11g in the *g-only* and *b/g modes*. The aim is to compare the expected IEEE 802.11g performance in theory to the observed performance in our experiments.

The 802.11 medium access control (MAC) uses *carrier sense multiple access with collision avoidance (CSMA/CA)* to facilitate shared medium access among several wireless devices that may want to communicate at the same time. Figure 10 illustrates the timing sequence involved in CSMA/CA. According to this automatic medium sharing, before a device starts transmission, it senses the channel to determine if it is idle. If the channel appears to be idle, it transmits its data frame after a short period of time known as the *Distributed Inter-Frame Space (DIFS)*. If the channel is busy, the device chooses a random value for its *Backoff* timer. This timer is frozen whenever the channel is busy. When the channel is sensed idle, it waits for *Backoff* timer to expire. When the timer expires and the channel is sensed to be idle, the station transmits its data frame and waits for an acknowledgment (Ack). *Short Inter-Frame Spacing (SIFS)*, which is smaller than DIFS, is the time interval between reception of a data frame and transmission of the corresponding Ack frame by destination. If the acknowledgment is received, the source station assumes that its data frame has been correctly received at the destination.

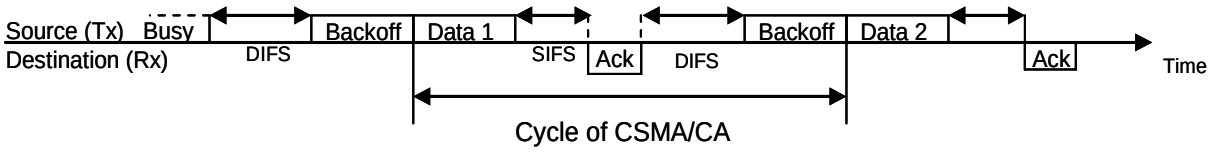

Figure 10: Timing diagram for CSMA/CA used in IEEE 802.11 protocols.

With this background, we will now derive the theoretical maximum achievable throughput (TMT) and minimum delay for IEEE 802.11g in both g-only and b/g modes. In the following calculations, we assume ideal conditions for packet transmission, i.e., there is no packet loss. We assume that a source device always has data to send. No management frames, e.g, beacon and association frames are taken into account. The standard distributed coordination function is used.

TMT = (MSDU size) / (Delay per MSDU) where *MSDU size* is the size of MAC service data unit defined as the length of the payload obtained by the MAC layer from the higher layer and *Delay per MSDU* = ($T_{DIFS} + T_{SIFS} + T_{BO} + T_{CTS} + T_{ACK} + T_{DATA}$)

Delay components for 802.11g only mode						
Scheme	T_{DIFS}	T_{SIFS}	T_{BO}	T_{CTS}	T_{ACK}	*TMT*
ERP-OFDM 6	28	10	67.5	-	50	$20+4\times\lceil(16+6+8\times(34+MSDU))/24\rceil+6$
ERP-OFDM 12	28	10	67.5	-	38	$20+4\times\lceil(16+6+8\times(34+MSDU))/48\rceil+6$
ERP-OFDM 24	28	10	67.5	-	32	$20+4\times\lceil(16+6+8\times(34+MSDU))/96\rceil+6$
ERP-OFDM 54	28	10	67.5	-	30	$20+4\times\lceil(16+6+8\times(34+MSDU))/216\rceil+6$
Delay components for 802.11b/g mode (with CTS-to-self protection)						
ERP-OFDM 6	50	10	150	203	50	$20+4\times\lceil(16+6+8\times(34+MSDU))/24\rceil+6$
ERP-OFDM 12	50	10	150	203	38	$20+4\times\lceil(16+6+8\times(34+MSDU))/48\rceil+6$
ERP-OFDM 24	50	10	150	203	32	$20+4\times\lceil(16+6+8\times(34+MSDU))/96\rceil+6$
ERP-OFDM 54	50	10	150	203	30	$20+4\times\lceil(16+6+8\times(34+MSDU))/216\rceil+6$

Table 2: Delay components and throughput (TMT) in *g-only* and *b/g modes*.

Setting the values for the various parameters as per the IEEE 802.11g standard (IEEE standard, 2003), we obtain the delay components for IEEE 802.11g and IEEE 802.11b/g as shown in Table 2. The *ERP-OFDM 6, 12, 24* and *54* represent the various modulation schemes defined in the standard.

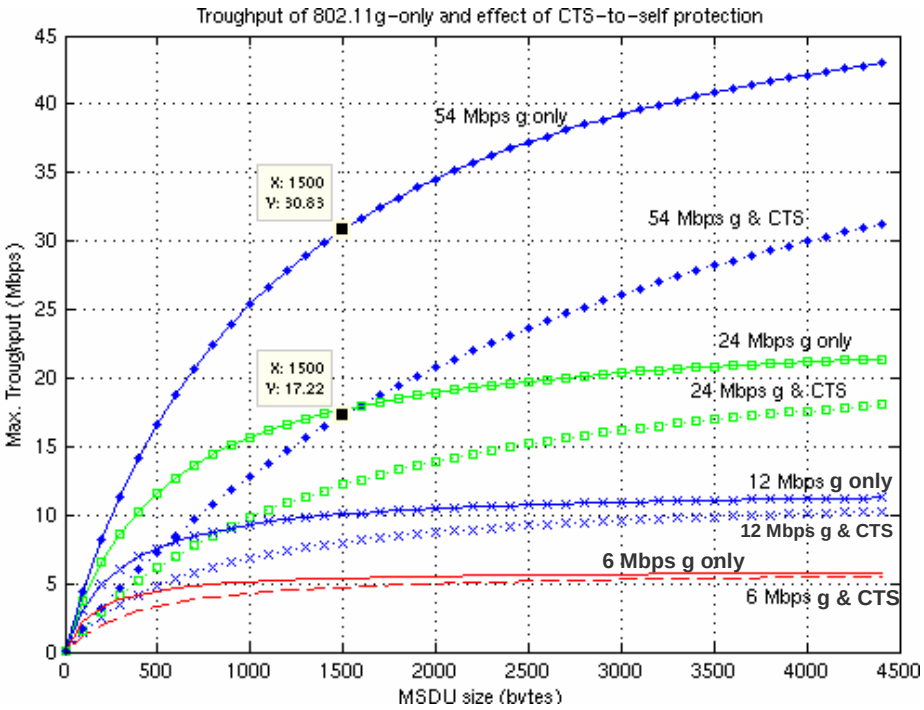

Figure 11: Theoretical maximum throughput (TMT) achievable using IEEE 802.11g-only and b/g modes.

Using the expression in Table 2, we plot the TMT as a function of MSDU in Figure 11. Comparing this with our experimental results, two things are evident. Due to the harsh conditions in the underground iron-ore mines, the network mostly operates in the 6 Mbps modulation scheme. With smaller MSDU, the degradation in throughput is much more in real life.

4. CONCLUDING REMARKS

In this paper, we presented our experimental study of an IEEE 802.11g network in LKAB's underground iron-ore mine in Kiruna, Sweden. Overall, our results hint that adopting wireless standards such as IEEE 802.11 in unconventional industrial environments should be done judiciously. Using measurements, we made an attempt to characterize the communication channel conditions in the mine, and study the network performance in terms of throughput, delay and packet loss ratio. The path loss characteristics in the mine were similar to those of a typical indoor office environment. However, the mine environment was found to be highly reflective causing multipath fading. This severely limited the maximum achievable data throughput in practice. We derived the theoretical throughput limits for IEEE 802.11g for comparison with our experimental results.

ACKNOWLEDGEMENTS

This work was partly funded by LKAB. We would like to thank the students: Magnus Armholt, Peter Engberg, Damien Mahinc, Veronica Nyberg, Thomas Renström, and Erik Rosenius at the Department of Computer Science and Electrical Engineering, Luleå University of Technology, for their contribution in the experimental study.

REFERENCES

IEEE standard 802.11g (2003) "Wireless LAN Medium Access Control (MAC) and Physical Layer (PHY) Specification: Further Higher Data Rate Extension in the 2.4 GHz Band" Available at: http://www.ieee.org.

Rappaport, T. (2001), Wireless Communications: Principles and Practice, Prenitce Hall PTR.

Henty, B. (2001) "Throughput Measurements and Empirical Prediction Models for IEEE 802.11b Wireless LAN (WLAN) Installations" Masters thesis, Department of Electrical and Computer Engineering, Virginia Polytechnic Institute and State University, 2001.